

Aerodynamic Stability Analysis of Two Heterogeneous UAVs in Close Formation Flight System

Johnson Yohannan¹, Imthias Ahamed T. P.²

¹Dept of EEE, UKF CET, Parippally, Kollam, Kerala & PhD Research Scholar, Kerala University, Kerala, India

²Dept of EEE, TKMCE, Kollam, Kerala, India

Email address:

j_yohannan2000@yahoo.com (J. Yohannan)

To cite this article:

Johnson Yohannan, Imthias Ahamed T. P. Aerodynamic Stability Analysis of Two Heterogeneous UAVs in Close Formation Flight System. *Fluid Mechanics*. Vol. 3, No. 3, 2017, pp. 13-19. doi: 10.11648/j.fm.20170303.11

Received: May 24, 2017; **Accepted:** June 5, 2017; **Published:** June 16, 2017

Abstract: The close formation flight of UAVs has many significant advantages over single vehicle flight. The aerodynamic stability analysis of two heterogeneous UAVs in close formation flight is detailed in the present paper. The issues of altitude changes and the associated shifts or changes in centre of gravity or moments, the equivalent actuator control surface deflections etc. are explained with the help of simulations. The short period frequency variations with these changes are also correlated with the help of pole-zero diagrams.

Keywords: Control, Close Formation Flight, Heterogeneous UAVs, Wing Vortex

1. Introduction

The Close Formation Flight (CFF) of Unmanned Aerospace Vehicles (UAVs) has diverse advantages such as fuel saving, cost reduction and preciseness in image capturing and data collection etc. The formation flight studies of heterogeneous Unmanned Aerial Vehicles (UAVs) in a stability analysis view point is hardly difficult to find. The proposed formation flight model in this paper consists of two members, namely 'leader' and 'follower'. The induced drag reduction caused by vortex effect of leader wing tips in close formation is made use of in this stability analysis work.

2. Literature Review

The most important control techniques used among available literature spanned over the last two decades are Intelligent Management Control Approach [1], Co-operative Control [2], Constraint Forces Approach [3], 3D Potential Field Approach [4], Co-operative tracking control [5], Constrained Adaptive Back-stepping Approach [6] and Vision based Scheme [7]. Proud, A. et al formulated PID feedback tracking control on two member system [8]. Dogan et al presented Linear Control Approach for formation reconfiguration [9]. Vanek and Balint applied Model

Predictive Control to real-time trajectory tracking of UAV formations [10]. Model Predictive Control Algorithm in non-linear dynamics is implemented by Saffarian and Fahimi [11]. The Decentralized Control Design Procedure for obstacle avoidance and collision is done by Haibo Min [12]. The aerodynamics associated with wing vortex effect and the resulting drag reduction is of special focus on the studies of F. Chichka et al. [13]. The simulation of aerodynamic cross-coupling vortex effects [14] is a useful reference for the present study.

After a brief review of relevant literature the stability analysis of two heterogeneous UAVs engaged in close formation flight and their associated aerodynamic interactions are detailed in section-III. The formation consensus of these UAVs from different altitude levels for drag reduction results in centre of gravity (c. g.) shifts and moment changes are quantitatively estimated and simulated in section-IV. These c. g. shifts and moment changes produces short period roots or frequency transitions, as illustrated by a pole-zero diagram at the end before conclusion. The aero stability analysis of the mechanical characteristics of two heterogeneous fixed-wing UAVs during a transformation to a close formation flight is highlighted in the present paper.

3. Aerodynamic Stability Analysis

When heterogeneous UAVs may enter into formation flight, their individual trim velocities, corresponding altitudes, atmospheric densities, trim angles of attacks etc. at which they are flying may be different. In order to make them fly at close formation benefitting the advantages of induced drag reduction, both should fly at least at the same altitude. If they can be placed at optimal longitudinal and lateral locations with respect to each other, maximum reduction of induced drag can be achieved.

The trim angle of attack (AOA), α_{trim} , in the trim (equilibrium) flight of a statically stable UAV is closely related with a definite value of lift coefficient C_{L_t} by the term $C_{L_t}\alpha_{trim}$. For the steady level flight of a UAV having weight W and wing area S at a particular altitude where its local atmospheric density is ρ_t , the corresponding (trim) velocity is [15]

$$V_t = \sqrt{\frac{2W}{\rho_t S C_{L_t} \alpha_{trim}}} \quad (1)$$

The trim velocities of two UAVs which are not identical in geometric and aerodynamic behavior will be different with respect to one another. A leader-follower formation flight pattern is assumed with one acting as the leader and the other as follower. The follower is made to bring to the leader's premises at first and then to make its speed equivalent to that of the leader so that the whole system is modeled in a close formation pattern. If their (trim) velocities at different altitudes are not equal, a change in (trim) AOA of the follower is necessary in order to offset the changes in dynamic pressure for a steady flight at the leader's altitude from the follower's original level.

Assume that the follower is initially moving with a trim velocity V_{ft} at a particular altitude where its local atmospheric density is ρ_{ft} at an AOA α_{fto} . It is made to track the leader having trim velocity V_{lt} with local density ρ_{lt} at a different level. The new AOA of the follower for maintaining steady flight at the leader's flight altitude is obtained from

$$\alpha_{ftn} = \left(\frac{V_{ft}}{V_{lt}}\right)^2 \left(\frac{\rho_{ft}}{\rho_{lt}}\right) \alpha_{fto} \quad (2)$$

The AOA change of follower results in non-zero moment creation about the centre of gravity (c.g.) around the trim AOA. The follower will deviate from its trim behavior at its new level. In order to bring back the follower into the trimmed flight, its moment coefficient, $C_{M,cg}$ versus AOA, α curve must be changed. Two methods are possible to achieve this change.

(i) Make the slope of moment coefficient versus AOA curve ($C_{M,cg}$ vs α) more negative such that $C_{M,cg} = 0$ at the new AOA, α_{ftn} (figure.1(a))

(ii) Changing the moment curve keeping the slope constant (figure.1(b)).

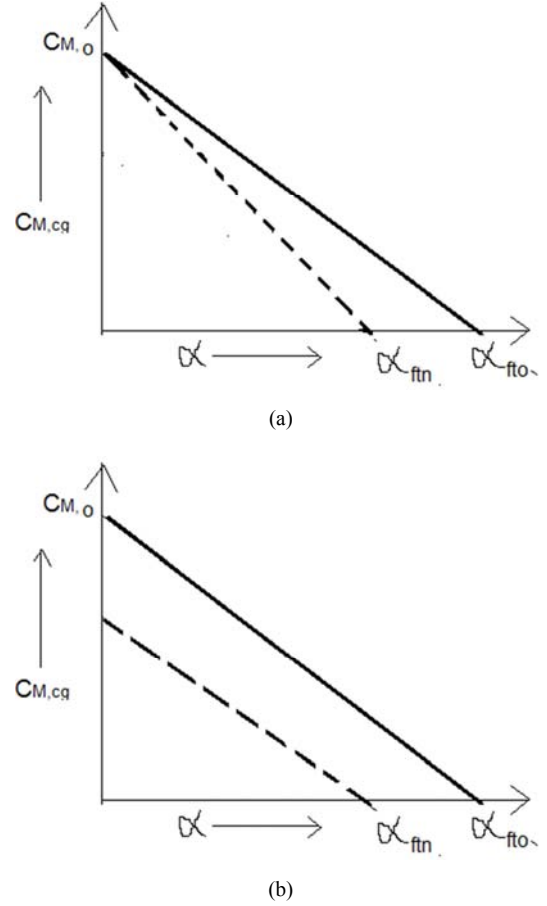


Figure 1. ((a) & (b)): Slope of moment coefficient versus AOA ($C_{M,cg}$ vs α) Curves.

The first method works on the basis of changing the slope of the curve. The only way to change the slope is to shift the centre of gravity either aft or forward towards the longitudinal axis, as evident from (3).

$$\frac{\partial C_{M,cg}}{\partial \alpha} = a \left[(h - h_{ac}) - V_H \frac{a_t}{a} \left(1 - \frac{\partial \epsilon}{\partial \alpha} \right) \right] \quad (3)$$

Where a - wing lift slope; a_t - tail lift slope; h & h_{ac} - co-ordinates of c.g. and aerodynamic centre (a.c.) respectively in fractions of chord length; $V_H = \frac{l_t S_t}{c S}$, horizontal tail volume ratio; l_t - tail moment arm; S_t - tail surface area; c - mean aerodynamic chord; S - wing area.

The tail dynamics is also taken into account here along with the wing dynamics. For the initial moment coefficient, $C_{M,cg}$ versus AOA, α curve (dashed line in figure.1)

$$\frac{\partial C_{M,cg}}{\partial \alpha \downarrow \alpha = \alpha_{fto}} = a \left[(h_{fto} - h_{ac}) - V_H \frac{a_t}{a} \left(1 - \frac{\partial \epsilon}{\partial \alpha} \right) \right] \quad (4)$$

For the changed $C_{M,cg}$ versus α curve (dotted line in fig.1)

$$\frac{\partial C_{M,cg}}{\partial \alpha \downarrow \alpha = \alpha_{ftn}} = a \left[(h_{ftn} - h_{ac}) - V_H \frac{a_t}{a} \left(1 - \frac{\partial \epsilon}{\partial \alpha} \right) \right] \quad (5)$$

Where h_{fto} and h_{ftn} are respectively centre of gravity coordinates in fractions of chord length at initial and changed conditions. Rearrange (4) and (5), then

$$h_{fto} - h_{ac} = \frac{\partial C_{M,cg}}{\partial \alpha} \Big|_{\alpha=\alpha_{fto}} * \frac{1}{a} + V_H \frac{a_t}{a} \left(1 - \frac{\partial \epsilon}{\partial \alpha}\right) \quad (6)$$

$$h_{ftn} - h_{ac} = \frac{\partial C_{M,cg}}{\partial \alpha} \Big|_{\alpha=\alpha_{ftn}} * \frac{1}{a} + V_H \frac{a_t}{a} \left(1 - \frac{\partial \epsilon}{\partial \alpha}\right) \quad (7)$$

As discussed earlier, h_{ac} is the aerodynamic centre coordinate in fraction of chord length. It can be expressed in terms of the neutral point coordinate, h_n . Since static stability is a function of h (either h_{fto} or h_{ftn} i. e. the location of centre of gravity in the longitudinal axis), any change in the centre of gravity location will change the static stability. By properly fixing the centre of gravity, the slope i.e., $\frac{\partial C_{M,cg}}{\partial \alpha}$ can be made more negative for stable operation. When the slope, $\frac{\partial C_{M,cg}}{\partial \alpha}$, becomes zero, $h = h_n$ (neutral point). The neutral point is located by putting $\frac{\partial C_{M,cg}}{\partial \alpha} = 0$ in (3) i.e.,

$$a \left[(h_n - h_{ac}) - V_H \frac{a_t}{a} \left(1 - \frac{\partial \epsilon}{\partial \alpha}\right) \right] = 0$$

$$h_n = h_{ac} + V_H \frac{a_t}{a} \left(1 - \frac{\partial \epsilon}{\partial \alpha}\right)$$

$$\text{Or } h_{ac} = h_n - V_H \frac{a_t}{a} \left(1 - \frac{\partial \epsilon}{\partial \alpha}\right) \quad (8)$$

The Static Margin (SM) for each case can be found out from the substitution of the value, h_{ac} from (8) in (6) & (7). The static margin is a direct measure of longitudinal static stability. It must be a positive quantity. Larger the static margin, more stable is the UAV. When the follower is in formation with the leader, the AOA of the follower α_{ftn} is increased by $\Delta\alpha_f$ such that the new value becomes

$$\alpha'_{ftn} = \alpha_{ftn} + \Delta\alpha_f \quad (9)$$

With the new increase in AOA, the fraction coordinate of centre of gravity, h_{ftn} , is changed to h'_{ftn} . Similar to the analysis used in (6) and (7) (refer figure 2)

$$h'_{ftn} - h_{ac} = \frac{\partial C_{M,cg}}{\partial \alpha} \Big|_{\alpha=\alpha'_{ftn}} * \frac{1}{a} + V_H \frac{a_t}{a} \left(1 - \frac{\partial \epsilon}{\partial \alpha}\right) \quad (10)$$

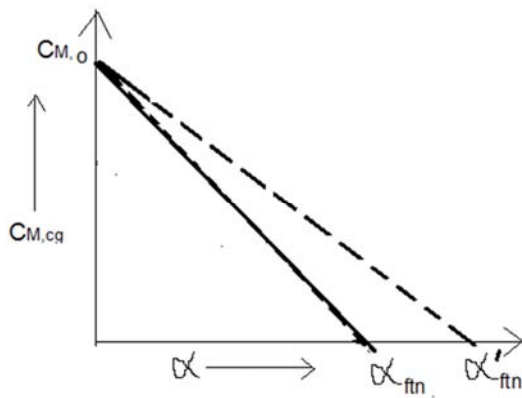


Figure 2. $C_{M,cg}$ vs α Curve.

With this new analysis, the static margin in the case of follower before and after the formation could be determined.

These static margin variations will be very useful in the stability analysis of formation flight systems. The moment change and the subsequent increase in lift force are the advantages gained to the follower in close formation flight. It is not easy to create these changes in a single UAV flight without the help of some control forces. The equivalent amount of control surface deflection required for the induced lift production in a formation flight can be calculated with the help of 2nd method stated in the previous section. The amount of elevator deflection required to move the AOA from α_{ftn} to α'_{ftn} , as depicted in fig. 3, can be calculated by recalling some aerodynamics basics associated with horizontal tail.

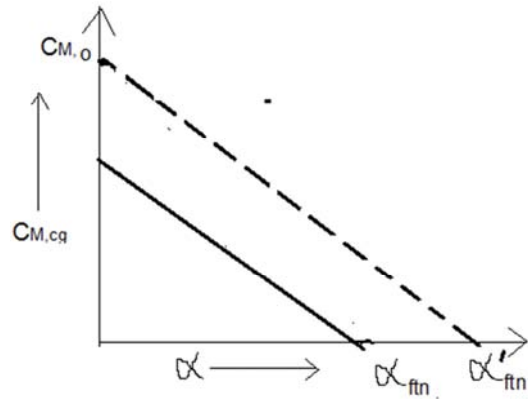


Figure 3. $C_{M,cg}$ vs α Curve.

The horizontal tail along with the elevator is assumed to be kept in neutral position (see figure 4 (a)). The tail is kept at an AOA α_t with no elevator deflection. The position of elevator is made to deflect, positive by convention, in downward direction by some means state through an angle δ_e as seen in figure 4 (b). The elevator control effectiveness, $\frac{\partial C_{L,t}}{\partial c}$, which is also positive, measures the control the elevator has empowered with. With the downward deflection of elevator, the lift coefficient $C_{L,t}$ versus α_t curve slope remains same and at the same time the change rate of $C_{L,t}$ with δ_e is also remaining constant.

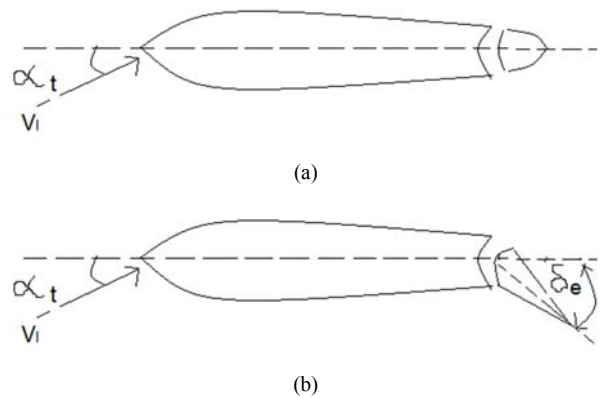


Figure 4. (a) With & (b) without elevator deflection.

The elevator deflection required to trim the follower UAV at new trim AOA and around the leader velocity is found out by

$$\delta_{trim} = \frac{C_{M,0} + \left(\frac{\partial C_{M,cg}}{\partial \alpha}\right) \alpha'_{ftn}}{V_H \left(\frac{\partial C_{L,t}}{\partial \delta_e}\right)} \quad (11)$$

Where

$$C_{M,0} = C_{M,acw} + V_H a_t (i_t + \epsilon_0) \quad (12)$$

$C_{M,0}$ - moment coefficient at zero AOA; i_t – tail setting angle

ϵ_0 -downwash angle when wing-body combination is at zero lift.

The centre of gravity shifting as explained in the first method is highly impractical. The moment curve change through control surface deflection is the only practical solution as the second method suggested. This is the principle behind the movement of follower to the leader's premises at the beginning of close formation flight.

Another problem faced in close formation analysis of non-identical UAVs is that the required data set of the follower flight at the leader's altitude may not be available. The actual available data of follower longitudinal flight dynamics may be at some other altitude or velocity which will be different from that of the leader. In such cases, available follower data must be changed in such a way as to suit with leader's altitude or velocity.

When considering the longitudinal state space data of UAVs, the dimensional stability and control derivatives such as $X_u, X_t, Z_u, Z_w, Z_q, Z_{\delta_e}, M_u, M_w, M_q$ and M_{δ_e} [16] depend on local atmospheric density and hence altitude as well as the longitudinal velocity. The proportionate changes in these two parameters are taken into consideration while changing the available data. The change in their stability and control derivatives is a result of change of centre of gravity of UAV and hence their associated moments. In other words the location of roots of the longitudinal dynamics and the centre of gravity location or pitching moment are related to each other. One can assess the interrelation between the centre of gravity change for formation configuration and the movement of roots of longitudinal dynamics in a pole-zero plot. The effects on both the short period and phugoid natural frequencies along with their damping ratios by the centre of gravity movement phenomenon are not in the same quantitative level. The short period mode is more affected by this phenomenon in its natural undamped frequency only and not in its damping ratio. The phugoid mode is affected more by its changed damped behavior with negligible change in frequency.

The movement of centre of gravity along fuselage can be forward or aft. The short period undamped natural frequency will be higher at forward centre of gravity than at aft centre of gravity by observing the following formula [17]

$$C_{m\alpha} = C_{L\alpha} (X_{cg} - X_{ac}) \quad (13)$$

The forward shift of centre of gravity increases X_{cg} and hence $C_{m\alpha}$. According to the least approximated formula for short period frequency, $\omega_{sp} = \sqrt{\frac{-C_{m\alpha} q_1 S \bar{c}}{I_{yy}}}$. The increased $C_{m\alpha}$ will surely increase the frequency.

All the above statements are proved and verified in the stability analysis of the given follower UAV in flight in the following section. The new trim AOA of the follower UAV required at the altitude level of leader flight path is obtained from the trim velocity equation below for steady level flight

$$V_{ft} = \sqrt{\frac{2W}{\rho_t S C_{L\alpha} \alpha_{ft0}}} \quad (14)$$

In steady level flight of the follower UAV both at its original trim steady level flight altitude and its proposed steady flight at the altitude level of leader, its body weight parameter for the above two conditions can be equated since it doesn't alter at these two conditions

$$\frac{V_{ft}^2 \rho_{t0} S C_{L\alpha} \alpha_{ft0}}{2} = \frac{V_{lt}^2 \rho_{tn} S C_{L\alpha} \alpha_{ftn}}{2} = W \quad (15)$$

where V_{ft} - follower velocity; V_{lt} - leader velocity; ρ_{t0}, ρ_{tn} - atmospheric densities at follower and leader altitude; $\alpha_{ft0}, \alpha_{ftn}$ - AOA of follower at its original and leader altitudes. In order to follow the leader by the follower in close formation, the follower must move with the formation speed. The leader speed is assumed as the formation speed for the present case. If the actual follower speed is less than the leader speed, then when they enter in close formation with balanced steady level flight, the lift coefficient C_{Lft0} , i.e. $C_{L\alpha} \alpha_{ft0}$ and hence the AOA α_{ft0} must be decreased such that the new AOA α_{ftn} is less than α_{ft0} . The corresponding change in pitching moment is required such that the value of $C_{M,cg}$ becomes zero at α_{ftn} . This pitching moment variation is made possible by changing the slope of $C_{M,cg}$ versus α curve. The forward shift in centre of gravity will make the slope more negative.

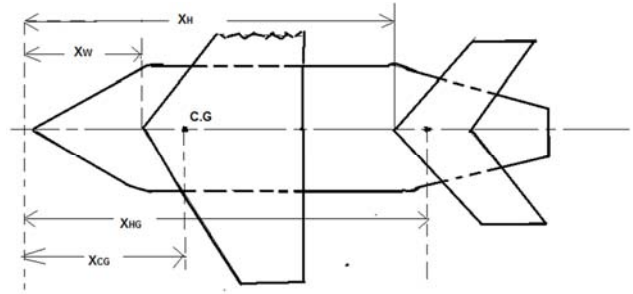


Figure 5. Measurements based on centre of gravity.

4. Simulation

The leader and the follower in the formation flight proposed for simulation are WVU YF-22 aircraft [18] and CONDOR Hybrid Electric Piloted Aircraft (HE-PRA) [19] respectively. Their geometrical and inertial data are given in Table-1 [18, 19]. The angle of attack of the follower at the level of altitude leader flight path, α_{ftn} , is calculated as 0.5° from the following values: leader velocity, $V_{lt} = 42 \text{ m/s}$; atmospheric density at follower altitude, $\rho_{t0} = 1.18 \text{ kg/m}^3$; atmospheric density at leader altitude, $\rho_{tn} = 1.21 \text{ kg/m}^3$; AOA of the follower at its original altitude, $\alpha_{ft0} = 3^\circ$.

Table 1. Geometrical and inertial data of UAVs.

Symbol	Quantity	Leader	Follower
b	Wing span	1.96m	4m
S	Wing area	1.37m ²	1.3m ²
AR	Aspect ratio	2.8	12
\bar{c}	Mean aerodynamic chord	0.76m	0.33m
M	Mass	20.64 kg	30 lb
V	Cruise speed	42 m/s	18 m/s
T	Thrust	54.62N	
α_{trim}	Angle of attack(trim)	3 ^o	0 ^o
θ_{trim}	Pitch angle(trim)	3 ^o	
I_{xx}	Moment of Inertia (M.I.)about roll axis	1.6kgm ²	3.884slug.ft ²
I_{yy}	M.I. about pitch axis	7.51kgm ²	1.572slug.ft ²
I_{zz}	M.I. about yaw axis	7.18kgm ²	4.569slug.ft ²

The neutral point location can be found out by setting the slope equals zero, i.e., $\frac{\partial C_{M,CG}}{\partial \alpha} = 0$ in (3), then $h = h_n$. The values of the parameters taken are: horizontal tail volume ratio $V_H = \frac{l_t S_t}{c S} = 0.47$ with l_t (tail moment arm) = 0.95 m; S_t (tail surface area) = 0.21m²; c (mean aerodynamic chord) = 0.33 m; S (wing area) = 1.3m²; aerodynamic centre coordinate in fraction of chord length, $h_{ac} = 1.13$; wing lift slope, $a = \frac{0.1}{deg}$; tail lift slope, $a_t = \frac{0.11}{deg}$; $\frac{\partial \epsilon}{\partial \alpha} = 0.48$. The calculated value of $h_n = 1.4$

The elevator deflection angle required to trim the follower UAV near the leader or formation velocity (42m/s) and at the leader altitude level (120m) from its original velocity (42m/s) and altitude (366m) is obtained from (11) as 1.6^o from the following

$$\frac{\partial C_{L,t}}{\partial \delta_e} = 0.04; C_{M,0} = 0.036 \text{ from } (12)$$

$$\frac{\partial C_{M,CG}}{\partial \alpha} = -0.012 \text{ (from graph)}$$

Thus in order to trim the follower UAV at the new AOA of 0.5^o from the initial trim AOA of 3^o, the elevator must be deflected downward by 1.6^o. The downward deflection of elevator is always taken as positive.

The first method explained in this section for bringing back the trimmed flight can be adopted here to get an idea of relative stability before and after the moment change.

Before moment change, (3) becomes

$$\frac{-0.036}{3} = 0.1[(h - h_{ac}) - 0.27] \quad (16)$$

After moment change

$$\frac{-0.036}{0.5} = 0.1[(h' - h_{ac}) - 0.27] \quad (17)$$

Since h_n is longer than h_{ac} by 0.27, then the Static Margin(SM), which is the difference between h_n and h_{ac} , before and after the moment change are 0.12 and 0.72 respectively. In other words the percentage increase in SM after centre of gravity shift is 50%. In physical measurement the centre of gravity is shifted by 18 cm forward with this SM increase.

Due to close formation effect the change in AOA of follower after it is moved close to the leader position is around

0.11^o. This becomes an advantage to the follower flight due to its induced lift contribution and drag reduction. This AOA change causes change in its pitching moment. The amount of centre of gravity shift due to this phenomenon only can also be calculated similar to the analysis done earlier. By referring (7) & (10) and fig.2, (18) and (19) are developed.

$$h_{ftn} - h_{ac} = \frac{-0.036}{0.5} * \frac{1}{0.1} + 0.27 = -0.45 \quad (18)$$

$$h'_{ftn} - h_{ac} = \frac{-0.036}{0.61} * \frac{1}{0.1} + 0.27 = -0.32 \quad (19)$$

Since h_n is longer than h_{ac} by 0.27, then static margins before and after the close formation effect are 0.72 and 0.59 respectively. The percentage decrease in SM after centre of gravity shift is 13%. In physical sense the centre of gravity is shifted by 4 cm aft due to the close formation effect. This centre of gravity shift and the corresponding pitch moment change is generated by the leader wing vortex effect only. There is no role played by the control surfaces in making these changes. Even then an equivalent amount of elevator deflection(which is not necessary for the present case) to this natural close formation effect can be calculated as in the previous analysis for study and analysis purpose only and its value is -0.07^o(refer (11)). The negative sign indicates that the elevator deflection is upward. The longitudinal dynamics state space data for the follower is given in (20).

$$\begin{bmatrix} \dot{u}_f \\ \dot{\alpha}_f \\ \dot{q}_f \\ \dot{\theta}_f \end{bmatrix} = \begin{bmatrix} -0.047 & 0.039 & 0.00 & -32.2 \\ -0.0374 & -4.592 & 50.8 & -0.01 \\ 0.0015 & -0.7248 & -2.96 & 0.008 \\ 0.000 & 0.000 & 1.000 & 0.000 \end{bmatrix} \begin{bmatrix} u_f \\ \alpha_f \\ q_f \\ \theta_f \end{bmatrix} + \begin{bmatrix} 0.000 & 0.038 \\ -0.14 & 0.000 \\ -28.126 & 0.000 \\ 0.000 & 0.000 \end{bmatrix} \begin{bmatrix} \delta_e \\ \delta_\tau \end{bmatrix} \quad (20)$$

Which is in the form $\dot{X} = AX + Bu$ where

$$A = \begin{bmatrix} -0.047 & 0.039 & 0.00 & -32.2 \\ -0.0374 & -4.592 & 50.8 & -0.01 \\ 0.0015 & -0.7248 & -2.96 & 0.008 \\ 0.000 & 0.000 & 1.000 & 0.000 \end{bmatrix}; B = \begin{bmatrix} 0.000 & 0.038 \\ -0.14 & 0.000 \\ -28.126 & 0.000 \\ 0.000 & 0.000 \end{bmatrix}; X = \begin{bmatrix} u_f \\ \alpha_f \\ q_f \\ \theta_f \end{bmatrix}; u = \begin{bmatrix} \delta_e \\ \delta_\tau \end{bmatrix} \quad (21)$$

The system states mentioned here are forward velocity(u_f), angle of attack(α_f), pitch rate(q_f) and pitch angle(θ_f). The control inputs are the elevator(δ_e) and throttle(δ_τ) deflections. All the dimensional stability and control derivatives in [A] and [B] matrix components are functions of dynamic pressure which by themselves are functions of local atmospheric density(altitude) and velocity. The follower UAV under consideration undergoes a steady level flight of velocity 17m/s at a height of 366m. When it enters into formation with the leader which flies steadily with 42m/s velocity at a level of 120m above ground, two important factors are needed to be modified in the present state space data. One is the ratio of two

velocities and the other one is the ratio of local atmospheric densities. The density ratio is very small as compared to the velocity ratio and can be assumed to neglect in practical considerations. All the other non-dimensional stability and control derivatives and geometric parameters like mass, area, wing area, chord length etc. will not undergo any variation in these transformations. The transformed [A] and [B] matrices i.e. A' and B' , at the leader height and speed level are

$$A' = \begin{bmatrix} -0.047 & 0.039 & 0.00 & -32.2 \\ -0.0374 & -4.592 & 50.8 & -0.01 \\ 0.0015 & -0.7248 & -2.96 & 0.008 \\ 0.000 & 0.000 & 1.000 & 0.000 \end{bmatrix}; \quad B' =$$

$$\begin{bmatrix} 0.000 & 0.038 \\ -0.14 & 0.000 \\ -28.126 & 0.000 \\ 0.000 & 0.000 \end{bmatrix} \quad (22)$$

The centre of gravity shift of the UAV discussed earlier is closely related with the oscillatory modes of the longitudinal dynamics. The oscillatory modes of initial and modified state space data of follower UAV in (21) and (22) can be determined from its Eigen values given below.

For [A]: $-3.6229 \mp i 5.9798 - 0.0101 \mp i 0.4278$

For [A']: $-8.4164 \mp i 13.9518 - 0.0486 \mp i 0.4249$

The first pair corresponds to the short period mode and the second one to phugoid mode. The pole-zero plot of both modes of [A] and [A'] is given in figure 6.

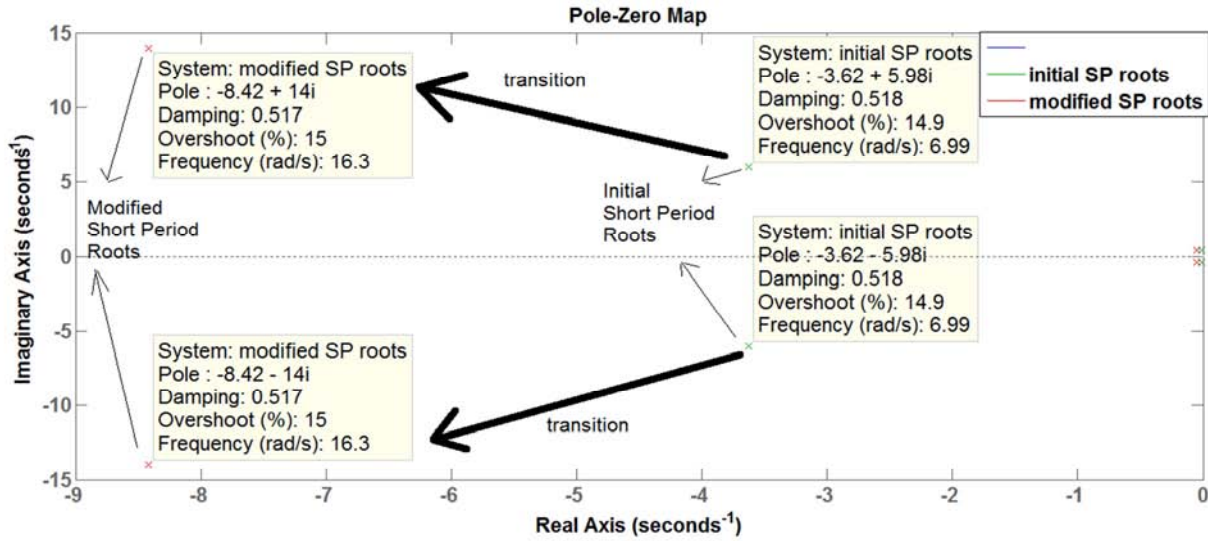


Figure 6. Pole-zero plot of the transition of short period roots of follower flight data from initial flight state to the altitude level of leader.

Since the real parts of all the roots above are negative, the system is dynamically stable. A comparison between short period and phugoid modes before and after the centre of gravity shift conditions is given in Table-2. The initial and modified follower flight state space data correspond to before and after centre of gravity shift respectively.

Table 2. Comparison between Phugoid and Short period modes [ω_n - undamped natural frequency in rad/sec; ξ - damping ratio; $t_{1/2}$ - time to half amplitude in seconds; P - period in seconds].

Oscillatory Modes		ω_n	ξ	$t_{1/2}$	P
SHORT PERIOD	Before c.g. shift	6.99	0.518	0.2	0.9
	After c.g. shift	16.29	0.516	0.08	0.4
PHUGOID	Before c.g. shift	0.428	0.02	68.6	14.67
	After c.g. shift	0.427	0.11	14.3	14.7

The centre of gravity shift produces frequency increase from 7rad/sec to 16.3rad/sec in short period mode and increase in damping ratio from 0.02 to 0.11 in phugoid mode. The short

period frequency approximation, i.e., $\omega_{nsp} = \sqrt{\frac{-C_{m\alpha}qS\bar{c}}{I_{yy}}}$ is applicable to the present case because (i) frequency will be higher in the case of forward centre of gravity (16.29rad/sec) than in the case of aft centre of gravity(6.99rad/sec) (ii) the

frequency will be higher at high speed (16.29rad/sec for 42m/s) than at low speed (6.99rad/sec for 17m/s)

5. Conclusion

The following conclusions can be drawn from the above stability analysis. When two heterogeneous UAVs at different altitudes and with different speeds may enter into formation flight with each other, then the

(i) change from trim angle of attack of follower UAV flight from one altitude to another is found out. This change is necessary to offset the dynamic pressure changes

(ii) centre of gravity shift (forward or aft) and the corresponding pitching moment change are found out.

(iii) ideal value of elevator control surface deflection required for moment change due to formation equivalent to the natural formation effect is found out.

(iv) transformation of follower UAV flight data at a different altitude and speed condition is made possible.

(v) relation between the short period frequency change and the centre of gravity shift or rate of pitching moment change is established through the stability analysis with the help of pole-zero plot.

Reference

- [1] Innocenti, M., Guilietti, F. and Pollini, L., "Intelligent Management Control for Unmanned Aircraft Navigation and Formation keeping," RTO AVT Course at Belgium, May, 2002.
- [2] How, J., King, E. and Kuwata, Y., "Flight Demonstration of cooperative control for UAV Teams," AIAA 3rd 'Unmanned Unlimited' Technical Conference, Workshop and Exhibit, Illinois, 2004.
- [3] Zou, Y. and Pagilla, P. R., "Distributed Formation Flight Control Using Constrained Forces," *Journal of Guidance, Control and Dynamics*, Vol 32, No. 1, 2009.
- [4] Paul T. R., Krogstad, and Gravdahl, J. T., "Modeling of UAV Formation Flight Using 3D Potential Field, Simulation Modeling Practice and Theory, Vol. 16, Issue 9, pp. 1453-1462, 2008.
- [5] S. Yoon, J. Bae, and Y. Kim, "Cooperative Standoff Tracking of a Moving Target using Decentralized Extended Information Filter," KSAS (Korean Society for Aeronautical and Space Science) Spring Conference, Gyeongju, Republic of Korea, Apr 2011.
- [6] S. Yoon, S. Park, and Y. Kim, "Constrained Adaptive Backstepping Controller Design for Aircraft Landing in Wind Disturbance and Actuator Stuck," *International Journal of Aeronautical and Space Sciences*, Vol. 13, No. 1, pp. 101-116, 2012.
- [7] H. J. Kim, M. Kim, H. Lim, C. Park, S. Yoon, D. Lee, G. Oh, J. Park, and Y. Kim, "Fully-Autonomous Vision-based Net-Recovery Landing System for a Fixed-Wing UAV," *IEEE/ASME Transactions on Mechatronics*, accepted for publication, 2013.
- [8] Proud, A., Pachter, M., and D'Azzo, J. J., "Close Formation Control," *Proceedings of the AIAA Guidance, Navigation, and Control Conference*, AIAA99-4207, pp. 1231 - 1246, Portland, OR, August 1999.
- [9] Dogan, A. and Venkataramanan, S., "Nonlinear control for Reconfiguration of Unmanned Aerial Vehicle Formation," *J. of Guidance, Control and Dynamics*, Vol 28, No 4 (2005).
- [10] Vanek and Balint, "Practical approach to real-time trajectory tracking of UAV formations," *Proceedings of the American Control Conference*, 2005.
- [11] Saffarian, M. and Fahimi, F., "Control of helicopters' formation using non-iterative nonlinear model predictive approach," *Proceedings of IEEE American Control Conference*, pp. 3707-3712, Seattle, Washington, June 2008.
- [12] Min, H., "Decentralized UAV formation tracking flight control using gyroscopic force," *IEEE International Conference on Computational Intelligence*, 2009.
- [13] Chichka, D. F., Speyer J. L., Fanti C. and Park C.G., "Peak seeking Control for Drag Reduction in Formation Flight," *AIAA Journal of Guidance, Control and Dynamics*, University of California, 2002.
- [14] Saban, D., Whidborne, J. F. and Cooke A., "Simulation of Wake Vortex Effects for UAV in close formation flight," *Aeronautical Journal*, Volume 113, Issue 1149, pp. 727-738, 2009.
- [15] Anderson J. D., "Introduction to Flight," 2nd Edition, McGraw Hill Book Company.
- [16] Johnson, Y. and Dasgupta, S., "Robust Hurwitz Stability and Performance Analysis of H-Infinity Controlled Forward-Velocity Dynamics of UAVs in Close Formation Flight Using Bounded Phase Conditions in a Kharitonov Framework," *Journal of The Institution of Engineers (India)*, Springer Publications, Series C: Volume 95, Issue 3 (2014), Page 223-231.
- [17] Roskam J., "Airplane Flight Dynamics and Automatic Flight Control," Part-I, DAR Corporation, USA, 2003.
- [18] Campa G., and Gu Y., "Design and flight testing of non-linear formation control law," *Science Direct, Control Engineering Practice* 15, 1 (2007).
- [19] Christopher, G., "Modeling, Simulation and Flight Test for Automatic Flight Control of the CONDOR Hybrid- Electric Remote Piloted Aircraft," MS Thesis Aeronautics and Astronautics Graduate School of Engineering and Management, Air Force Institute of Technology Air University, March, 2012.